

# Stability on Adaptive NN Formation Control with Variant Formation Patterns and Interaction Topologies

**Xin Chen and Yangmin Li**

Department of Electromechanical Engineering, Faculty of Science and Technology,  
University of Macau, Av. Padre Tomás Pereira S.J., Taipa, Macao SAR, P. R.China  
ya27407@umac.mo & ymli@umac.mo

**Abstract:** The formation task achieved by multiple robots is a tough issue in practice, because of the limitations of the sensing abilities and communicating functions among them. This paper investigates the decentralized formation control in case of parameter uncertainties, bounded disturbances, and variant interactions among robots. To design decentralized controller, a formation description is firstly proposed, which consists of two aspects in terms of formation pattern and interaction topology. Then the formation control using adaptive neural network (ANN) is proposed based on the relative error derived from formation description. From the analysis on stability of the formation control under invariant/variant formation pattern and interaction topology, it is concluded that if formation pattern is of class  $C^k$ ,  $k \geq 1$ , and interaction graph is connected and changed with finite times, the convergence of the formation control is guaranteed, so that robots must form the formation described by the formation pattern.

**Keywords:** adapted neural network control, interaction topology, Lyapunov theorem for nonsmooth systems, switched system.

## 1. Introduction

Multiple robots coordination to form a kind of pattern is an interesting phenomenon, which also has wide applications in highway transportation, army inspection, and external stars exploration. If a predetermined formation pattern is given, a group of robots forming formation will be investigated in this paper.

Formation is viewed as a kind of information consensus in which robots or agents interact with each other using various sensors and communication techniques. For example, a simple discrete-time Vicsek model is built up, which commands a group of robots to move on the plane with the same heading (Vicsek, T., Czirok, A., Jacob, E. B. & Schochet, O., 1995). Using graph theory, the theoretical explanation about Vicsek model and its extended version are provided in (Jababaie, A., Lin, J. & Morse, A. S., 2003) and (Ren, W. & Beard, R. W., 2005).

In robotic applications, there are several approaches to multiagent coordination referred in the literature, namely leader-following, behavioral, potential fields, virtual structures, and generalized coordinates.

In leader-following, one of the agents is designated as the leader, which tracks predefined reference trajectories, with the rest of the members designated as followers which follow the leader or their neighbors (Wang, P. K. C., 1991, Sugar, T. & Kumar, V., 1998, Desai, J. P., Ostrowski, J. & Kumar, V., 1998). Leader-following paradigm is easy to understand and implement. In addition, the formation can still be maintained even if the leader is perturbed by

some disturbances. However there is no explicit feedback to the formation.

The virtual structure approach is another technique widely used in formation control, where the entire formation is treated as a single structure (Lewis, M. A. & Tan, K.H., 1997, Moscovitz, Y. & DeClaris, N., 1998, Tan, K.H. & Lewis, M.A., 1996). Using virtual structure approach, it is easy to prescribe a coordinated behavior for the group. And feedback to the virtual structure is naturally defined. Hence even if some agents are failed, the formation is still maintained. However this approach is not proper when formation is time-varying or needs to be frequently reconfigured.

A general approach is developed to model and control of formations in terms of generalized coordinates (Spry, S. C., 2002, Spry, S. & Hedrick, J. K., 2004). It produces asymptotic tracking of trajectories, including those with time-varying rotations and shape, and allows the controller to be formulated in terms of quantities which are closely related to the performance objectives of tracking a group trajectory while maintaining a desired formation shape.

All three techniques mentioned above require that the full state of the leader or virtual structure be communicated to each member of the formation. In contrast, behavior-based approach is decentralized and may be implemented with less communication. The basic idea of the behavioral approach is to prescribe several desired behaviors for each agent, such as target seeking, collision/obstacle avoidance, and interaction with

neighbors, so that desirable group behavior emerges finally (Jonathan, R. T., Beard, R. W. & Young, B. J., 2003, Balch, T. & Arkin, R. C., 1998, Chen, Q. & Luh, J. Y. S., 1994). As a decentralized implementation, behavioral approach enables agents derive controls for multiple competing objectives simultaneously. In addition, there is explicit feedback to the formation. The primary shortage is that group behavior cannot be explicitly defined. Hence it is difficult to analyze group behavior mathematically.

Another decentralized approach of formation control is potential fields approach (Schneider, F. E. & Wildermuth, D., 2003). In this method, different virtual forces belonging to robots, obstacles and the desired shape of formation are combined and used to move each robot to its desired position inside the formation. Similar to behavioral approach, the control derived based on several forces enables agents form a formation, while avoiding collision with obstacles or others. But the formation pattern (shape) needs to be broadcasted to all members. Hence comparing with behavioral method, it needs more communication cost. Moreover, for mobile robots with nonholonomic constraints, it is difficult to provide a mechanism to solve special movements induced by nonholonomic constraints.

Just as mentioned, leader-follower approach is easily implemented in practice. Comparing with virtual structure approach, leader-follower paradigm can realize time-varying formation pattern. Even under complex conditions, such as uncertain parameters and unknown disturbances, individual control in leader-following paradigm can guarantee formation stability. Hence it is easily realized in practical applications than generalized coordinates. Comparing with behavioral approaches, the feasibility of leader-following paradigm can be guaranteed mathematically. Therefore in this paper, we adopt leader-follower to realize formation in which information exchange is directed, and robots are required to form formation according to certain formation patterns. The major problem is to develop a decentralized control strategy to guarantee formation's stability.

To describe formation behavior in the continuous-time case, a technique of leader-to-formation stability (LFS) is proposed in which formation stability is analyzed by input-to-state stability method (Tanner, H. G., Pappas, G. J. & Kumar, V., 2004). Another important technique broadly used for formation control stability is Lyapunov theory (Liu, Y., Passino, K. M. & Polycarpou, M., 2001, Ogren, P., Egerstedt, M. & Hu, X., 2002, Kowalczyk, W. & Kozłowski, K., 2004, Bicho, E. & Monteiro, S., 2003, Balch, T. & Hybinette, M., 2000).

Since in practical situations, most platforms of formation are constructed using multiple nonholonomic mobile robots which are always modeled with some uncertain parameters, and because of limitations on sensors and communication ability, relationship among robots described by formation patterns and interaction topology is always variant, the linear feedback-control law

proposed in (Tanner, H. G., Pappas, G. J. & Kumar, V., 2004) can not be employed for the formation. Hence we extend the ANN control designed for smooth continuous system (Fierro, R. & Lewis, F. L., 1998, Lewis, F. L., Yegildirek, A. & Liu, K., 1996) to the case of nonsmooth, even noncontinuous systems, so that the control strategy is able to make robots keep in regular formation in practical environment.

The rest of this paper is organized as follows. In Section 2, we introduce the description about formation structure using graph theory. Based on the description, Section 3 presents the sufficient condition of formation control in terms of a Lemma. Section 4 introduces the decentralized control strategy using adaptive neural network. Three theorems are presented in Section 5 to investigate the feasibility of this formation control under different conditions, including variant or invariant formation pattern and interaction topology. The feasibility is validated by a simulation, and some discussions about practical applications are provided. Finally conclusions are drawn in Section 6.

## 2. Description of Formation's Internal Information

In this paper, a group of robots are labeled by  $R_i$  ( $i=1, \dots, N$ ), where  $R_i$  represents the leader of the formation. Let  $P^d = [p_1^d \ p_2^d \ \dots \ p_N^d]^T$  denote the desired positions of all robots relative to robot  $l$ . Obviously,  $p_l^d = 0$ . Let  $P = [p_1 \ p_2 \ \dots \ p_N]^T$  denote the coordinates of robots in universal frame. The internal information of a formation consists of two aspects.

### (1) Formation pattern (denoted by $D^d(t)$ )

Formation pattern describes the desired formation shape by a matrix,  $D^d = \{D_{ij}^d\}_{N \times N}$ , whose elements present all desired relative distances between the robots, i.e.,  $D_{ij}^d = p_i^d - p_j^d$ . Obviously  $D_{ii}^d = 0$ . Moreover we denote  $D^d(t)$  as the time-varying formation pattern. We also let  $D = \{D_{ij}\}_{N \times N}$  denote real relative distances between robots, where  $D_{ij} = p_i - p_j$ . Fig. 1 shows an example of relative matrix  $D^d$ . In the example,  $R_1$  is assigned to play the role of the formation leader.

### (2) Interaction topology (denoted by $G$ )

To detect the relative positions within a formation, robots need to make contacts with each other. Hence it needs to describe interactions among robots. No matter what technique is applied to realize interaction, we use graph theory to present interactions among robots.

A directed graph  $G$  is exploited to describe the interaction topology of formation, which consists of a set of vertices (robots)  $\Xi$  and a set of arcs  $\Omega$ , where  $\alpha = (v, w) \in \Omega$  and  $v, w \in \Xi$ . Arc  $\alpha(v, w)$  represents that  $R_v$  takes  $R_w$  as a reference object to compute its desired

reference position. Since a robot may interact with several robots simultaneously, its reference position may be determined by several robots. Let  $G = \{g_{ij}\}_{N \times N}$  denote adjacency matrix associated with graph  $G$ , where  $g_{ij}$  represents a kind of weight denoting the degree of  $R_j$  affecting the reference position of  $R_i$ .  $G$  has a property,

$$\sum_{j=1}^N g_{ij} = 1. \quad (1)$$

And we define  $H = \{h_{ij}\}_{N \times N}$  as  $H = I - G$ . Due to the property of  $G$ , it holds that  $\sum_{j=1}^N h_{ij} = 0$ .

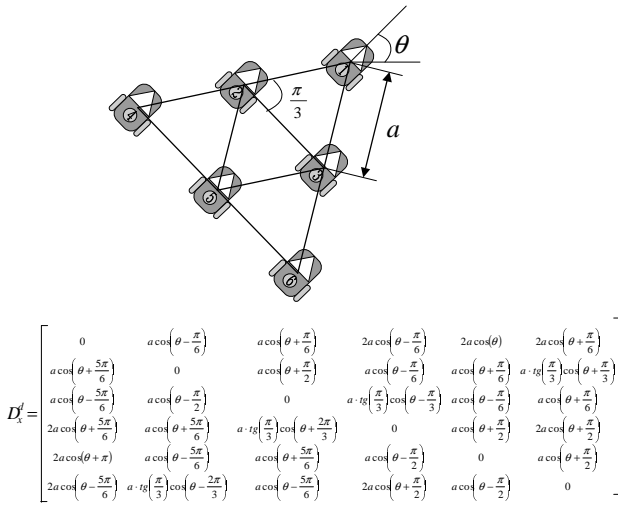


Fig. 1. A formation pattern including six robots. Only the x-axis coordinate of  $D^d$  is displayed below the figure

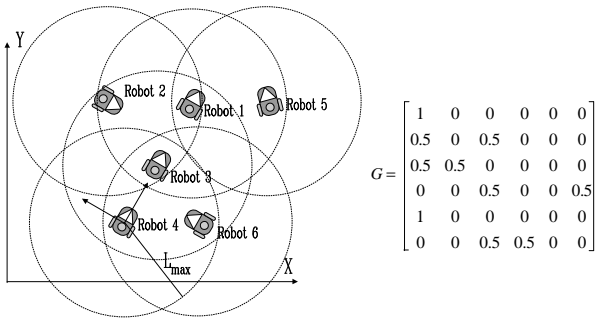


Fig. 2. An example of interaction topology among six robots, where  $L_{max}$  represents the maximal range of interaction, so that a robot can make contact with other robots within this range

An example of interaction topology and adjacency matrix is illustrated in Fig. 2. Since  $R_1$  plays the role of the leader, it holds that  $g_{11} = 1$ , while other diagonal entries are zero  $g_{ii} = 0, (i = 2, \dots, N)$ .

Obviously combining these two aspects, the internal information of a formation can be described by  $G \circ D^d$ , where the operator  $\circ$  means Hadamard product (to simplify denotation, we let  $D^d$  denote both time-fixed and time-varying formation patterns).

### 3. Motivation of Formation Control

Based on the description of formation, let  $E = \{e_j\}_{N \times 1} = (G \circ D - G \circ D^d)1_{N \times 1}$  be a relative error vector, so that it follows that

$$E = HP - G \circ D^d 1_{N \times 1} = P - (GP + G \circ D^d 1_{N \times 1}) \quad (2)$$

Since  $R_l$  plays the role of the formation leader, it holds  $g_{ll} = 1$ , while  $g_{ij} = 0, j = 1, \dots, N$ , and  $j \neq l$ . Therefore the  $l$ th element of the relative error,  $e_l$ , equals zero. It's reasonable because the adjacency graph is built relative to the leader, the relative error of  $R_l$  should be zero.

The following lemma is introduced.

**Lemma 1.** Given an error shown in (2), if the adjacency matrix  $G$  is connected, when  $E = 0$ , all robots will follow the leader of the formation and form a formation described by  $D^d$  (or  $D^d(t)$ ).

*Proof:* See Appendix A.1.

Lemma 1 suggests a way to realize formation control. Since  $GP + G \circ D^d 1_{N \times 1}$  in (2) can be measured on real time, if  $G$  and  $D^d$  are known for all members of the formation, every robot can control itself to follow a reference point determined by  $GP + G \circ D^d 1_{N \times 1}$  in order to form formation.

### 4. Individual Control Strategy

#### 4.1. Dynamic Description of Individual Robot

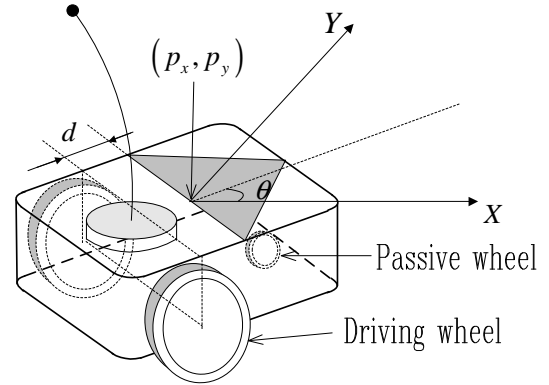


Fig. 3. A two-wheel-driven mobile robot.

A kind of two-wheel car-like mobile robot shown in Fig. 3 is employed to realize formation. The dynamics of robot is expressed as

$$M(q)\ddot{q} + V(q, \dot{q})\dot{q} + \tau_d = J^T(q)\lambda + B(q)\tau, \quad (3)$$

where  $q = [p_x \ p_y \ \theta]^T$  represents general coordinate,  $\tau_d$  represents bounded disturbance and unmodeled dynamics. We take the center of mass as the robot's position. Matrices referred in the equation are given by

$$M(q) = \begin{bmatrix} m & 0 & md \sin \theta \\ 0 & m & -md \cos \theta \\ md \sin \theta & -md \cos \theta & I_0 + md^2 \end{bmatrix},$$

$$\tau = [\tau_l \quad \tau_r]^T, V(q, \dot{q}) = \begin{bmatrix} 0 & 0 & md \dot{\theta} \cos \theta \\ 0 & 0 & md \dot{\theta} \sin \theta \\ 0 & 0 & 0 \end{bmatrix},$$

$$B = \frac{1}{r} \begin{bmatrix} \cos \theta & \cos \theta \\ \sin \theta & \sin \theta \\ L & -L \end{bmatrix}, J(q) = [\sin \theta \quad -\cos \theta \quad d].$$

Normally the nonholonomic constraints can be expressed as  $J(q)\dot{q} = 0$  or  $\dot{p}_x \sin \theta - \dot{p}_y \cos \theta + d\dot{\theta} = 0$ . Then the second order derivative of  $\theta$  is expressed as:

$$\ddot{\theta} = \frac{1}{d}(\ddot{p}_y \cos \theta - \ddot{p}_x \sin \theta) + \frac{1}{2d^2}(\dot{p}_x^2 - \dot{p}_y^2) \sin 2\theta - \frac{1}{d^2} \dot{p}_x \dot{p}_y (\cos^2 \theta - \sin^2 \theta). \quad (4)$$

It is easy to find a full rank matrix  $A(q)$  which is formed by the vectors spanning the null space of constraint matrix  $J(q)$  such that  $A^T(q)J^T(q) = 0$ , where

$$A(q) = \begin{bmatrix} \cos \theta & -d \sin \theta \\ \sin \theta & d \cos \theta \\ 0 & 1 \end{bmatrix}. \text{ Multiplying both sides of (3)}$$

with  $A^T$  to eliminate nonholonomic constraint forces  $\lambda$ , it follows that

$$A^T M(q) \ddot{q} + A^T V(q, \dot{q}) \dot{q} + \bar{\tau}_d = A^T B(q) \tau, \quad (5)$$

where  $\bar{\tau}_d = A^T \tau_d$ . If define  $p = [p_x \quad p_y]^T$ ,

$$T = \begin{bmatrix} \cos \theta & \sin \theta \\ -\sin \theta & \cos \theta \end{bmatrix} \text{ and } M_c = \begin{bmatrix} m & 0 \\ 0 & \frac{1}{d} \end{bmatrix}, \quad (5) \text{ can be}$$

transformed to

$$M_c T \ddot{p} + M_c \dot{T} \dot{p} = A^T B \tau - \bar{\tau}_d. \quad (6)$$

#### 4.2. Neural Network Controller

Following (2), we take  $GP + G \circ D^d 1_{N \times 1}$  as local desired position for individual control design. If we decompose  $GP + G \circ D^d 1_{N \times 1}$  for individual robots, the desired

reference point for  $R_i$  is of the form  $p_i^d = \sum_{j=1}^N g_{ij}(p_j + D_{ij}^d)$ .

Therefore we define the individual relative position error as

$$e_i = p_i - p_i^d = p_i - \sum_{j=1}^N g_{ij}(p_j + D_{ij}^d). \quad (7)$$

A filtered error is defined as  $z_i = \dot{e}_i + \Lambda e_i$ . If define a temporal variable,  $\dot{p}_i^r = \dot{p}_i^d - \Lambda e_i$ , then  $z_i = \dot{p}_i - \dot{p}_i^r$ . Substitute it into (6), and let  $\tilde{z}_i = T z_i$ , thus

$$M_c \tilde{z}_i = A^T B \tau_i - \bar{M}_i \ddot{p}_i^r - \bar{V}_i \dot{p}_i^r - \bar{\tau}_{id}. \quad (8)$$

$$\text{where } \bar{M}_i = \begin{bmatrix} m_i & 0 \\ 0 & \frac{1}{d_i} \end{bmatrix} \begin{bmatrix} \cos \theta_i & \sin \theta_i \\ -\sin \theta_i & \cos \theta_i \end{bmatrix},$$

$$\bar{V}_i = \frac{1}{d_i} (\dot{x} \sin \theta_i - \dot{y} \cos \theta_i) \begin{bmatrix} m_i & 0 \\ 0 & \frac{1}{d_i} \end{bmatrix} \begin{bmatrix} \sin \theta_i & -\cos \theta_i \\ \cos \theta_i & \sin \theta_i \end{bmatrix}.$$

Because there may exist parameter uncertainties, we use a neural network to model  $\bar{M}_i \ddot{p}_i^r + \bar{V}_i \dot{p}_i^r$  on-line.

A nonlinear function  $f(X_i) = \bar{M}_i \ddot{p}_i^r + \bar{V}_i \dot{p}_i^r$  is defined in which  $X_i = [\dot{p}_i \quad \sin \theta_i \quad \cos \theta_i \quad \ddot{p}_i^r \quad \dot{p}_i^r]^T$ . To simplify the expression, the subscript  $i$  is omitted. We suppose that there exists a two-layer feedforward NN like Fig. 4 shows which can approximate  $f(X)$ , i.e.

$$f(X) = W^T \sigma(V^T X) + \varepsilon, \quad (9)$$

where  $V \in R^{N_I \times N_H}$  represent the input-to-hidden-layer interconnection weights,  $W \in R^{N_H \times N_O}$  represent the hidden-layer-to-outputs interconnection weights, where  $N_H$ ,  $N_I$  and  $N_O$  are the numbers of neurons in the hidden layer, the input layer, and the output layer respectively, the activation function  $\sigma(\cdot)$  is in the form of  $\sigma(x) = \frac{1}{1+e^{-x}}$ ,  $\varepsilon$  is the NN functional approximation error.

Let  $Y_M$  denote the bound of ideal weights, such that  $\|W\|_F + \|V\|_F \leq Y_M$ .

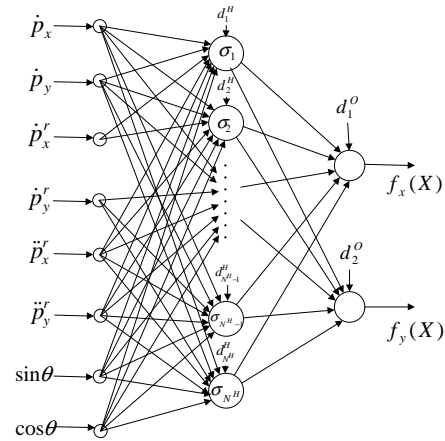


Fig. 4. A two-layer feedforward neural network

Firstly, there is a property about the bounding fact.

*Property 1:*  $X$  is bounded by

$$\|X\| \leq c_1 \Phi + c_2 \|\tilde{z}\| + c_3, \quad (10)$$

where  $c_1$  to  $c_3$  are positive scalars,  $\Phi$  is the bound which will satisfy

$$\left\| \begin{bmatrix} p^d \\ \dot{p}^d \\ \ddot{p}^d \end{bmatrix} \right\| \leq \Phi. \quad (11)$$

*Proof:* See Appendix A.2.

The purpose of NN learning is to construct a NN function  $\hat{f}(X)$  to estimate  $f(X)$  on-line, which can be written as

$$\hat{f}(X) = \hat{W}^T \sigma(\hat{V}^T X), \quad (12)$$

where  $\hat{W}$  and  $\hat{V}$  are estimates of NN weights.

The estimated errors are defined as  $\tilde{f} = f - \hat{f}$ ,  $\tilde{W} = W - \hat{W}$ , and  $\tilde{V} = V - \hat{V}$ . And the hidden-layer output error is defined as  $\tilde{\sigma} = \sigma - \hat{\sigma} = \sigma(V^T X) - \sigma(\hat{V}^T X)$ .

Applying Taylor series expansion, we can obtain

$$\sigma(V^T X) = \sigma(\hat{V}^T X) + \sigma'(\hat{V}^T X) \tilde{V}^T X + O(\tilde{V}^T X)^2, \quad (13)$$

where  $\sigma'(\hat{y}) = \frac{\partial \sigma(y)}{\partial y} \Big|_{y=\hat{y}}$ . Therefore,

$$\tilde{\sigma} = \sigma'(\hat{V}^T X) \tilde{V}^T X + O(\tilde{V}^T X)^2, \quad (14)$$

where  $O(\tilde{V}^T X)^2$  satisfies the following property.

*Property 2:*

$$\|O(\tilde{V}^T X)^2\| \leq c_4 + c_8 \|\tilde{V}\|_F \|\tilde{z}\| + c_9 \|\tilde{V}\|_F. \quad (15)$$

where  $c_4$ ,  $c_8$ , and  $c_9$  are positive scalars.

*Proof:* See Appendix A.3.

Substituting  $f(X)$  into (8), we have

$$M_c \dot{\tilde{z}} = A^T B \tau - f(X) - \bar{\tau}_d = A^T B \tau - W^T \sigma(V^T X) - \bar{\tau}_d + \varepsilon. \quad (16)$$

Now we design the input-output feedback linearization controller in terms of (17) and the adaptive backpropagation learning algorithm in terms of (18) respectively. Consequently the architecture of formation control is shown in Fig. 5.

$$\tau = (A^T B)^{-1} (\hat{W}^T \sigma(\hat{V}^T X) - K\tilde{z} + \gamma), \quad (17)$$

$$\dot{\hat{W}} = F \hat{\sigma}' \hat{V}^T X \tilde{z}^T - F \hat{\sigma} \tilde{z}^T - \kappa F \|\tilde{z}\| \hat{W}, \quad (18)$$

$$\dot{\hat{V}} = -UX (\hat{\sigma}' \hat{W} \tilde{z})^T - \kappa U \|\tilde{z}\| \hat{V},$$

where  $K = \text{diag}\{k_1, k_2\}$  in which  $k_1$  and  $k_2$  are positive scalars,  $\gamma$  is a robust control term to suppress the disturbance of unmodeled structure of dynamics  $\tau_d$  and functional approximation error of NN  $\varepsilon$ ,  $F$  and  $U$  are positive definite design parameter matrices governing the speed of learning.

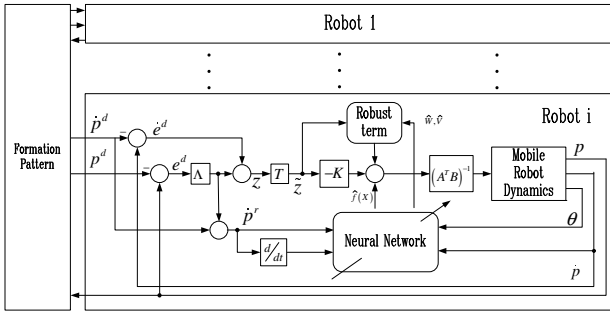


Fig. 5. The architecture of formation control

Substitute the control law into (16), and let  $\sigma$  and  $\hat{\sigma}$  denote  $\sigma(V^T X)$  and  $\sigma(\hat{V}^T X)$  respectively, thus

$$M_c \dot{\tilde{z}} = -K\tilde{z} - W^T \sigma + \hat{W}^T \hat{\sigma} + \gamma - \bar{\tau}_d + \varepsilon. \quad (19)$$

Adding and subtracting  $W^T \hat{\sigma}$  and  $\hat{W}^T \tilde{\sigma}$ , and using (13) and (14), we have

$$M_c \dot{\tilde{z}} = -K\tilde{z} - \tilde{W}^T (\hat{\sigma} - \hat{\sigma}' \hat{V}^T X) - \hat{W}^T \tilde{\sigma}' \tilde{V}^T X + s + \gamma, \quad (20)$$

where  $s(t)$  is a disturbance term,

$$s(t) = -\tilde{W}^T \hat{\sigma}' V^T X - W^T O(\tilde{V}^T X) - \bar{\tau}_d + \varepsilon. \quad (21)$$

## 5. Stability on Formation Control

In Section 2, it is mentioned that there are two aspects, the formation pattern  $D^d$  and interaction matrix  $G$ , describing the information within a formation. In practice, due to the different requirements about formation tasks, formation pattern and interaction topology may be invariant or variant respectively. In this section, the stability of the formation control under three different situations covering all possible kinds of formation pattern and interaction topology will be analyzed.

### 5.1. Stability under Invariant Formation Pattern and Invariant Interaction Topology

The words "invariant formation pattern" in the title means that during the process, the formation pattern  $D^d$  is constant, or the desired formation shape is static. The following theorem describes the convergence of formation control with fixed formation pattern.

**Theorem 1:** Assume that for a multi-robot system designed for formation task with a predetermined leader, formation pattern is fixed, and adjacency matrix associated with interaction graph is strong connected and invariant. If there are bounded disturbance and parameter uncertainty about robot structure, the robots must form a formation using individual control strategy represented in (17) and (18).

*Proof:* See Appendix A.4.

**Remark 1:** It should be mentioned that the proof of convergence does not assert that the weight error  $\tilde{W}$  and  $\tilde{V}$  will converge to zero. That means although  $\hat{f}(X)$  approaches to  $f(X)$ , the  $\hat{W}$  and  $\hat{V}$  may not converge to the desired weights  $W$  and  $V$  without error eventually. But since for a formation task, the most important thing is to keep a formation shape, it is acceptable that there exist estimated errors on NN weights.

The simulation of a formation with fixed formation pattern is proposed, where six robots are required to form a hexagon formation. The size of robot is  $0.14 \times 0.08m$ , while its weight is  $1kg$ . The NN used in individual control includes a hidden layer with 40 nodes. All weights of NN are initialized as random values within  $[0,1]$ .  $R_1$  plays the role of formation leader, which is required to follow a trajectory expressed as  $p_y^d = 0.3 \sin(p_x^d \pi)$ . The simulation results are shown in Fig. 6. From Fig. 6 (a), we observe that six robots scattering randomly at the beginning can form a formation. The invariant interaction topology is denoted by arrows shown in the figure (a). And Fig. 6 (b) shows the relative errors of robots, where  $e_x$  and  $e_y$  mean the relative errors in X-axis and Y-axis directions respectively. Obviously all errors converge to zero in the end. So the individual control strategy works very well.

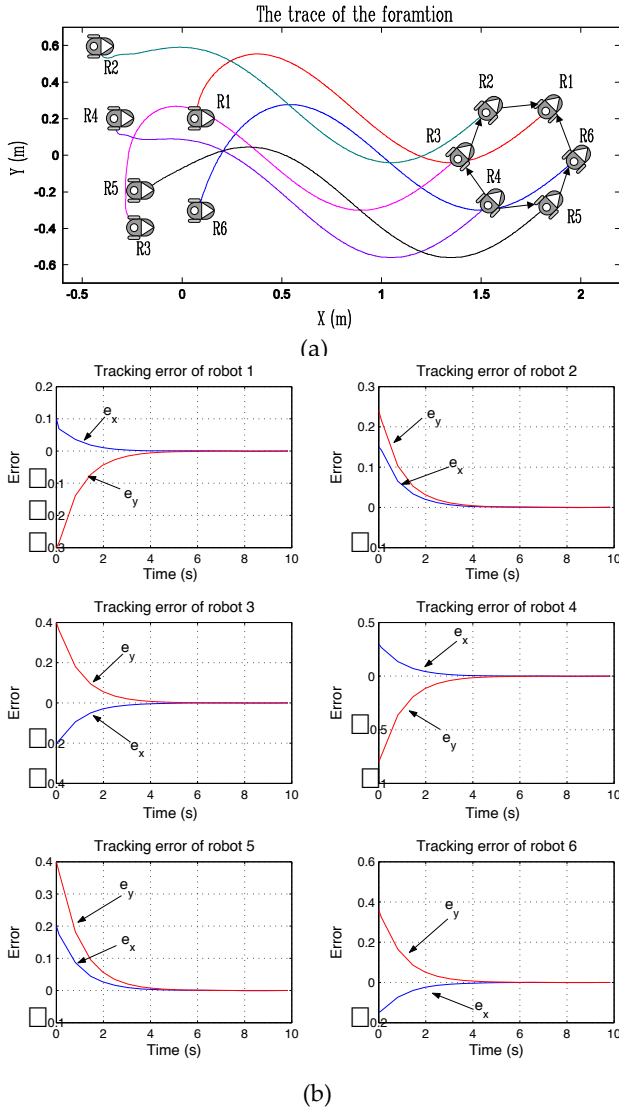


Fig. 6. Simulation results of fixed formation pattern and interaction topology

## 5.2. Stability under Variant Formation Patterns and Invariant Interaction Topology

The variant formation pattern means that the formation pattern is changed over time. Just as mentioned in Section 2, the time-varying formation pattern is denoted by  $D^d(t)$ .

### 5.2.1. The Problem Induced by Variant Formation Pattern

In practice, due to moving obstacles, perceiving limits, and even direct control commands, formation pattern should be changed on real time. For example, when a formation is passing through an obstacle field, if the formation perceives an obstacle which is on the way of its members, it has to generate another formation pattern so that its members can avoid the obstacle according to the new formation pattern. A simple illustration about the change of formation pattern is shown in Fig. 7 where there are two robots forming a leader-follower formation. When it is perceived that the obstacle is on the way of  $R_2$ ,  $R_2$  has to change its relative position from parallel to  $R_1$

to behind  $R_1$ . Hence a transition process, which is between the dashed verticals in Fig. 7, is necessary to make formation pattern change continuously. It is obvious that since the formation pattern is changed on real time,  $D^d(t)$  over the whole process must be not of class  $C^\infty$ , i.e.,  $D^d(t)$  doesn't have continuous derivatives of any order, so that we can not guarantee the convergence of formation control using Theorem 1. To ensure convergence of the formation control, we have to figure out the conditions under which the adaptive NN control can be applied. Theorem 2 presents the conditions which ensure stability of formation control.

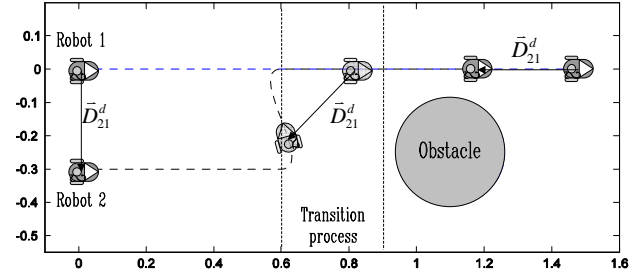


Fig. 7. An example of variant formation pattern

### 5.2.2. Convergence of Formation Control with Variant Formation Pattern

**Theorem 2:** If all assumptions are the same as Theorem 1 except that formation pattern is time-varying and  $D^d(t)$  is of class  $C^k$ ,  $k \geq 1$ , the robots must converge to the formation pattern using individual control strategy represented in (17) and (18).

*Proof:* See Appendix A.5.

From Theorem 2, it is concluded that the sufficient condition of convergence of the formation with invariant interaction topology is that the formation pattern is at least of class  $C^1$  continuous.  $\odot$

**Remark 2:** Now we can propose a practical strategy to generate a transition process in order to make formation pattern be of class  $C^1$ .

Assume that within the duration of  $[t_1, t_2]$ , formation pattern is required to change from  $D_1^d(t)$  to  $D_2^d(t)$ , which is of class  $C^\infty$  respectively. The transition process is defined as

$$\psi(t) = \eta(t)D_1^d(t) + (1 - \eta(t))D_2^d(t). \quad (22)$$

where  $t \in [t_1, t_2]$ ,  $\eta(t)$  is a function which satisfies the following boundary conditions.

$$\eta(t_1) = 1, \eta(t_2) = 0, \left. \frac{d\eta(t)}{dt} \right|_{t=t_1} = \left. \frac{d\eta(t)}{dt} \right|_{t=t_2} = 0, \quad (23)$$

Applying the transition process  $\psi(t)$ , it is easy to prove that the formation pattern  $D^d(t)$  described in (24) is of class  $C^1$ .

$$D^d(t) = \begin{cases} D_1^d(t), & t < t_1, \\ \psi(t), & t \geq t_1, t < t_2, \\ D_2^d(t), & t \geq t_2. \end{cases} \quad (24)$$

Hence such a general transition process ensures that the pattern satisfies the conditions in Theorem 2, so that the formation must be constructed. The simulation proposed in the next subsection includes an example of such transition process.

### 5.3. Stability under Variant Interaction Topology

#### 5.3.1. Noncontinuous System Resulting from Variant Interaction Topology

Since interaction is affected by the robot's ability such as perceiving range and communication bandwidth, one robot is able to make contact with other robots within its perceiving range. If the distance between robots become too far to set up interactions, or their interactions are blocked by obstacles, robots have to seek other partners to set up new interactions. Therefore the interaction topology and the graph associated with it may change from time to time. That means the adjacency matrix is variant.

Based on the analysis of the previous subsection, it is known that the system errors,  $\tilde{z}$ ,  $\tilde{w}$ , and  $\tilde{v}$  should be smooth continuous, in order that the NN control strategy be applied. Assume that the adjacency matrix is changed from  $G_1$  to  $G_2$ . It is easily proved that even if the formation pattern and positions of robots are fixed, the relative errors  $E$  associated with the two adjacency matrices are different. That means when  $G$  is changed, there is a sudden change of  $\tilde{z}$ , so that  $\tilde{z}$  is not continuous any more, and the control strategy can not be expressed in the Filippov sense. In fact we can not guarantee the convergence of formation control with variant interaction topology only using Theorems 1 and 2. Hence in this subsection, we analyze performance of formation control using theory of switched systems, in order to figure out the additional conditions for formation control.

#### 5.3.2. The Extended Theorem about Convergence of Switched System

Owing to change of interaction topology, the formation system can be viewed as a switched system. Theorem 2.3 in (Branicky, M. S., 1998) asserts that in a switched system, if dynamics of all subsystems are Lipschitz continuous and there is a Lyapunov-like function for the system, the system must be stable. But due to robust term  $\gamma$ , if the subsystems are chosen according to (Branicky, M. S., 1998) implied, the dynamics of subsystems in formation control are not Lipschitz continuous. Hence we need to propose an extended theorem based on Theorem 2.3 in (Branicky, M. S., 1998) to analyze stability of formation control with variant interaction topology.

Similar to (Branicky, M. S., 1998), for a switched system  $\dot{x}(t) = f_j(x(t), t)$ ,  $j \in Q$ , where  $Q$  represents a set including all systems to which we can switch, we define the infinite switching sequence that indexed by an initial state,  $x_0$ :

$$S = x_0; (k_0, t_0), (k_1, t_1), \dots, \quad (25)$$

where  $(k_s, t_s)$  means that the system evolves according to  $\dot{x}(t) = f_{k_s}(x(t), t)$  for  $t_s \leq t \leq t_{s+1}$ . We also define the sequence of indexes

$$\pi_1(S) = x_0; k_0, k_1, \dots, \quad (26)$$

and the sequence of switching times

$$\pi_2(S) = x_0; t_0, t_1, \dots. \quad (27)$$

The interval completion  $I(T)$  of a nondecreasing sequence of times  $T = t_0, t_1, \dots$  is the set  $\bigcup_{k \in \mathbb{Z}^+} [t_{2k}, t_{2k+1}]$ . Different from the definition in (Branicky, M. S., 1998), here  $T$  is not required to be strictly increasing. That means there exist times  $t_k$ ,  $k \in \mathbb{Z}^+$  satisfying  $t_k = t_{k+1}$ . If let  $S|j$  denote the endpoints of the times that system  $j$  is active,  $I(S|j)$  represents the set of times that the  $j$ th system is active. Let  $\varepsilon(T)$  denote the even sequence of  $T: t_0, t_2, t_4, \dots$ . Based on these definitions, we extend Theorem 2.3 in (Branicky, M. S., 1998) with slight modifications to get the following theorem.

**Theorem 3:** Suppose that there are vector fields  $\dot{x} = f_j(x)$  with  $f_j(0) = 0$ ,  $j \in Q$ , where  $Q$  represents a set including all systems to which we can switch, and the size of  $Q$  is finite. Let  $S$  be the set of all switching sequences associated with the system. Suppose that for each  $S \in S$  and for all  $j$ ,  $L_j$  is positive definite function (p.d.f.) for  $f_j$  over  $S|j$  and satisfies these two properties:

1.  $L_j(0) = 0$ ,  $\dot{L}_j(x(t)) \leq 0$  for all  $t \in I(S|j)$ ;
2.  $L_j$  is almost nonincreasing on  $\varepsilon(S|j)$  except finite times in finite duration.

Then the system is stable in the sense of Lyapunov.

*Proof:* See Appendix A.6.

It is obvious that if there is a Lyapunov-like function satisfying the properties mentioned in Theorem 3, the stability of the formation control must be guaranteed. In the following subsection, we will analyze the properties of our formation system to verify their stability in practical conditions.

#### 5.3.3. Stability of Formation Control with Variant Interaction Topology

We denote set  $\mathbf{G} = \{G_i : i = 1, 2, \dots, N_G\}$  which consists of all possible connected adjacency matrices. Obviously equation  $H_i P^d = G_i \circ D^d \mathbf{1}_{N \times 1}$  has identical solution  $P^d$  for all  $G_i \in \mathbf{G}$ . An error is defined as  $\bar{E} = [\bar{e}_1 \ \dots \ \bar{e}_N]^T$ , where  $\bar{e}_i = p_i - p_i^d$ . Since  $E = H\bar{E}$ , if  $\lim_{t \rightarrow \infty} \bar{E}(t) = 0$ , robots must form a formation with pattern  $D^d$  according to Lemma 1.

Since the definition of  $\bar{E}$  does not include  $H$ ,  $\bar{E}$  must be continuous, even if  $G$  is changed over time. Based on it, another filter error is defined as  $\bar{Z} = [\bar{z}_1 \ \dots \ \bar{z}_N]^T = \bar{E} + \bar{\Lambda}\bar{E}$ , where  $\bar{\Lambda} = \text{diag}\{\Lambda_i\}$ .

If define  $\tilde{\mathbf{W}} = [\tilde{w}_1^T \ \tilde{w}_2^T \ \dots \ \tilde{w}_N^T]^T$  and  $\tilde{\mathbf{V}} = [\tilde{v}_1^T \ \tilde{v}_2^T \ \dots \ \tilde{v}_N^T]^T$ , the formation system can be

expressed as a switched system in terms of (28).

$$\begin{aligned}\dot{\bar{Z}} &= f_{1j}(\bar{Z}, \bar{\tilde{W}}, \bar{\tilde{V}}), \\ \dot{\bar{\tilde{W}}} &= f_{2j}(\bar{Z}, \bar{\tilde{W}}, \bar{\tilde{V}}), \\ \dot{\bar{\tilde{V}}} &= f_{3j}(\bar{Z}, \bar{\tilde{W}}, \bar{\tilde{V}}),\end{aligned}\quad (28)$$

where  $j \in Q$ . The elements included in  $Q$  will be explained later.

Before determining Lyapunov-like function, we firstly propose all situations which result in switch, in order that  $f_{1j}$ ,  $f_{2j}$ , and  $f_{3j}$ , where  $j \in Q$ , are globally Lipschitz continuous.

- 1) Due to effect of the robust term  $\gamma$ , when  $\bar{z}$  passes through zero, (20) is not Lipschitz continuous. So we prescribe that there is a switch at this instant. According to the definition of the robust term, the forms of  $f_{1j}$ ,  $f_{2j}$ , and  $f_{3j}$  before and after this switch are the same and Lipschitz continuous respectively. That means such switch does not change system index  $j$ .
- 2) When the transition strategy shown in Section 5.2 is applied to make  $D^d \in C^1$ , from the discussions in the previous subsection, we know that the learning algorithm (18) is not Lipschitz continuous. We also prescribe at this instant that a switch is triggered. And similar to the previous situation, this switch does not change system index  $j$ .
- 3) When interaction topology is changed, due to noncontinuity of relative errors, the system index  $j$  is switched to another one. Since the size of  $\mathbf{G}$  is finite, there are finite systems corresponding to all connected interaction topologies in  $\mathbf{G}$ .

From these situations, we know that only the third situation induces change of system index, so the size of  $Q$  is the same as the size of  $\mathbf{G}$ . Hence there are finite systems included in the switched system.

Consider one system included in  $Q$ . To simplify denotation, the index  $j$  is omitted. Since  $R_l$  is the leader of the formation, it holds that  $\bar{z}_l(t) = 0$  for all  $t$ . To design a positive definite function (p.d.f.) in Theorem 3, we delete all entries which relate to robot  $l$  from  $\bar{Z}$ ,  $\bar{\tilde{W}}$ , and  $\bar{\tilde{V}}$ . Consequently we let  $\hat{Z} = [\bar{z}_1 \cdots \bar{z}_{l-1} \bar{z}_{l+1} \cdots \bar{z}_N]^T$ ,  $\hat{\tilde{W}} = [\bar{\tilde{w}}_1^T \cdots \bar{\tilde{w}}_{l-1}^T \bar{\tilde{w}}_{l+1}^T \cdots \bar{\tilde{w}}_N^T]^T$  and  $\hat{\tilde{V}} = [\bar{\tilde{v}}_1^T \cdots \bar{\tilde{v}}_{l-1}^T \bar{\tilde{v}}_{l+1}^T \cdots \bar{\tilde{v}}_N^T]^T$  denote these reduced states. Then a p.d.f. is defined as

$$L = \frac{1}{2}[(\hat{T}\hat{H}\hat{Z})^T \hat{M}(\hat{T}\hat{H}\hat{Z}) + \text{tr}\{\hat{\tilde{W}}^T \hat{F}^{-1} \hat{\tilde{W}}\} + \text{tr}\{\hat{\tilde{V}}^T \hat{G}^{-1} \hat{\tilde{V}}\}], \quad (29)$$

where  $\hat{T} = \text{diag}\{T_i\}$ ,  $\hat{M} = \text{diag}\{M_{ci}\}$ ,  $\hat{F} = \text{diag}\{F_i\}$ ,  $\hat{G} = \text{diag}\{G_i\}$ ,  $i = 1, \dots, N, i \neq l$ ,  $\hat{H}$  denotes the matrix resulting from taking off the both  $l$ th row and column of  $H$ . Undoubtedly it holds that  $L(0) = 0$ .

From (1), it holds that  $\sum_{k=1, k \neq l}^N h_{ik} = -h_{il}$ , and  $h_{lk} = 0$ .

Therefore the following equality holds.

$$(\hat{T}\hat{H}\hat{Z})^T \hat{M}(\hat{T}\hat{H}\hat{Z}) = (\hat{T}\hat{H}\hat{Z})^T \hat{M}(\hat{T}\hat{H}\hat{Z}),$$

where  $\bar{H}$  denotes the submatrix of  $H$  which results from taking off the  $l$ th row of  $H$ . Substitute it into (29).

$$L = \frac{1}{2}[(\hat{T}\hat{H}\hat{Z})^T \hat{M}(\hat{T}\hat{H}\hat{Z}) + \text{tr}\{\hat{\tilde{W}}^T \hat{F}^{-1} \hat{\tilde{W}}\} + \text{tr}\{\hat{\tilde{V}}^T \hat{G}^{-1} \hat{\tilde{V}}\}], \quad (30)$$

Obviously (30) is the combination of the Lyapunov functions in the form of (A.4.1) for all robots except robot  $l$ . Therefore after some computations similar to the derivation of (A.4.12) which represents the derivative of individual Lyapunov function, for each  $j \in Q$ , we have

$$\begin{aligned}\dot{L}_j &\leq -(\hat{T}\hat{H}_j\hat{Z})^T \bar{K}_{\min}(\hat{T}\hat{H}_j\hat{Z}) - \sum_{i=1, i \neq l}^N \kappa \|\bar{z}_i\| \left( \|\bar{\tilde{y}}_i\|_F - \frac{C_3}{2} \right)^2 \\ &\leq -\hat{K}_{\min} \|\hat{T}\hat{H}_j\hat{Z}\|^2 - \sum_{i=1, i \neq l}^N \kappa \|\bar{z}_i\| \left( \|\bar{\tilde{y}}_i\|_F - \frac{C_3}{2} \right)^2 \\ &\leq -\hat{K}_{\min} \|\hat{T}\hat{H}_j\hat{Z}\|^2 - \kappa \min_{0 \leq i \leq N} \left\{ \left( \|\bar{\tilde{y}}_i\|_F - \frac{C_3}{2} \right)^2 \right\} \|\hat{T}\hat{H}_j\hat{Z}\| \leq 0,\end{aligned}\quad (31)$$

where  $\bar{K}_{\min} = \text{diag}\{K_i^{\min}\}$  and  $\hat{K}_{\min} = \min\{K_i^{\min}\}$ ,  $i = 1, \dots, N$ ,  $i \neq l$ , where  $K_i^{\min}$  is the minimum singular value of  $K_i$ . Therefore  $L_j$  satisfies the first property of p.d.f. in Theorem 3.

Now let's check whether  $L_j$  satisfies the second property of p.d.f. or not. Suppose in a duration  $[t_{\text{start}}, t_{\text{end}})$  there is no switch induced by change of interaction topology. Since the first two situations inducing switches do not change system index  $j$ , the switch sequence in the duration can be denoted by  $S_d = x_{t_{\text{start}}}; (j, t_0), (j, t_1), \dots, (j, t_k), \dots$ , where  $t_0 = t_{\text{start}}$ ,  $t_k \leq t_{\text{end}}$ . According to the analysis in Sections 5.1 and 5.2, in  $[t_{\text{start}}, t_{\text{end}})$ , the formation system is a nonsmooth continuous system, and  $L_j$  is monotonically nonincreasing on  $S_d$ . That means the situation 1) and 2) can not make  $L_j$  be increasing on  $\varepsilon(S|j)$  in the interval  $[t_{\text{start}}, t_{\text{end}})$ . So the only chance that  $L_j$  is increasing on  $\varepsilon(S|j)$  is induced by the situation 3), the change of interaction topology, while not every time of change of interaction topology induces an increase of  $L_j$  on  $\varepsilon(S|j)$ . Therefore to guarantee the second property of p.d.f. in Theorem 3, it is required that there are finite changes about interaction topology, in order that the system is stable in the sense of Lyapunov. Moreover after the last time of the change of interaction topology, the system becomes the nonsmooth continuous system analyzed in the previous subsections, so that  $Z$  must converge to zero, and robots will form a formation.

In one word, if interaction topology is changed finite times, the formation system must satisfy the conditions mentioned in Theorem 3, so that according to Theorem 3, it is guaranteed that the group of robots must form a formation described by the pattern  $D^d(t)$ .

**Remark 3:** In practice, the situations which induce change of interaction topology normally include obstacles blocking,



limits of perceiving range, and communication. If obstacle field is bounded, there exists a finite time  $t_F$  after which the interaction topology stops changing. Hence the property 2 in Theorem 3 is easily satisfied in practice.

#### 5.4. Simulation about Formation Control with Variant Formation Pattern and Interaction Topology

We propose a simulation to illustrate the performance of the formation when formation pattern and interaction topology are variant. In the simulation, a formation navigation based on particle swarm optimization (PSO) is utilized to generate proper paths for the leader of the formation in order that other members can follow the leader to pass through an obstacle field without collision with obstacles. Roughly speaking, in the simulation there are two formation patterns applied: a triangle one and a linear one. If no obstacles perceived by the leader, the group tries to keep a triangle formation. Once the leader senses obstacles, it generates a proper path to avoid obstacles. At the same time, it changes the formation pattern to a linear one, so that other robots will follow the "footprints" of the leader to avoid obstacles.

Since the simulation is mainly to verify the feasibility of control strategy, the details of the process of path planning using PSO is ignored, which can be found in (Li, Y. & Chen, X., 2005). In the simulation,  $R_1$  plays the leader of the formation. There are some assumptions about the simulation.

- The maximum of sensor range for obstacles is 0.7m;
- The maximum of interaction range between robots is 0.6m;
- Four obstacles are located at (2.5,0.25) , (3.5,0.5) , (4.5,-0.3) , and (5.5,0.1) .

The parameters about robots are the same as the simulation presented in Section 5.1. The transition function  $\eta(t)$  used in the simulation is of the form

$$\eta(t) = 0.5 + 0.5 \cos\left(\frac{t-t_0}{t_D} \pi\right), \quad (32)$$

where  $t_D$  is the duration of the transition process;  $t_0$  is the beginning of the transition process.

The results of simulation are illustrated in Fig.8 and Fig.9. The whole path generated for the leader includes four segments, two beelines and two curves. According to these segments, the whole formation process is also divided into four segments which are denoted by 1 to 4 in Fig. 8 (a). The segments of path designed for  $R_1$  in segments 2 and 3 are expressed as following.

##### 1) Segment 2

$$p_y^d = 0.0089(p_x^d)^5 - 0.1863(p_x^d)^4 + 1.4295(p_x^d)^3 - 4.8848(p_x^d)^2 + 7.2954(p_x^d) - 3.9011;$$

##### 2) Segment 3

$$p_y^d = 0.0157(p_x^d)^5 - 0.3468(p_x^d)^4 + 2.8763(p_x^d)^3 - 11.0097(p_x^d)^2 + 19.2293(p_x^d) - 12.0840.$$

Obviously the whole path generated for  $R_1$  is smooth

continuous. If it is assumed there is a virtual point moving along the path, the leader uses the adaptive NN to follow this virtual point to reach the destination.

Fig. 8 (b) displays the change of formation pattern and interaction topology. The arrows shown in (b) indicate the interaction topologies among robots. Due to the interaction limits 0.6m, at the beginning an interaction topology is set up as (i). And such topology is held until the formation enters segment 2. When the formation becomes a linear one, because  $R_3$  is beyond the interaction limit of  $R_4$ ,  $R_4$  has to change its reference objects. The similar situation happens to  $R_5$ . Hence the interaction topology is changed to the form shown in (iii), which is held as far as the end of the simulation.

Fig. 8 (c) shows the relative errors of robots, all of them converge to zero. When the formation passes from segment 1 into segment 2 and from segment 3 into segment 4, two transition processes of formation pattern are employed to change  $D^d$  smoothly, which can be observed near 7.5 seconds and 35 seconds respectively. At these two instants, relative errors of  $R_2$  to  $R_6$  increase.

That looks against the convergence of the system. We think this phenomenon is induced by the relative fast convergence of the estimate of weights. This quick change about estimate of weights can be observed in the right figure of Fig. 9 (b), in which at times near 7.5s and 35s, the trace of the estimate of NN weights of  $R_3$  decreases more quickly than other time.

Just as mentioned, when the formation changes from triangle one to linear one or vice versa, the relative errors become noncontinuous. That induces a sudden change of relative error, which is called a leap of error. Fig.8 (d) illustrates the leaps of error of  $R_4$  and  $R_5$ , when  $R_4$  and  $R_5$  have to change their reference objects. Obviously if formation is formed, such leaps of errors are so trivial relative to the size of robots, that the effect of noncontinuity induced by time-varying  $G$  can be ignored in practice.

Since the optimal values of weights can not be obtained, we only display the comparison of the output of  $\hat{f}(X)$  with the actual result of  $\bar{M} \ddot{p}^r + \bar{V} \dot{p}^r$  in Fig. 9 (a). Here only the NNs of  $R_1$  and  $R_3$  are picked as examples. From the figure it is observed that at the beginning of the process the outputs of NN and  $\bar{M} \ddot{p}^r + \bar{V} \dot{p}^r$  are almost the same. It implies that the estimates of weights converge to the optimal values of NN model. In fact Theorem 1 has asserted that the estimates of NN need not converge to the desired weights. Even if NN learning converges to suboptimal solution, robots are still able to form a formation.

Finally Fig. 9 (b) displays the temporal dynamics of  $\text{trace}(\hat{W}^T \hat{W}) + \text{trace}(\hat{V}^T \hat{V})$ .

**Remark 4:** Although the formation control works well in the simulation, when it is applied in practical system, the

adaptive control can not avoid collision among robots by itself. Such phenomenon is observed in Fig. 6 and Fig. 8, shortly after beginning, the traces of robots intercross with each other, it implies that there is a danger of collision among robots. Hence in practical applications, the control strategy proposed in this paper is more suitable for the situation, where robots are initially localized near the formation pattern, in order to avoid collisions within the transient process. It looks like a limitation about such leader-following approach. But once formation is nearly constructed, the adaptive NN control will guarantee accurate control of all robots. And from the simulation, it is observed that even if formation pattern is time-varying, the relative errors are all limited within a small range which is far less than the size of robots. Hence once formation is formed, the adaptive control is powerful enough to avoid collision within formation.

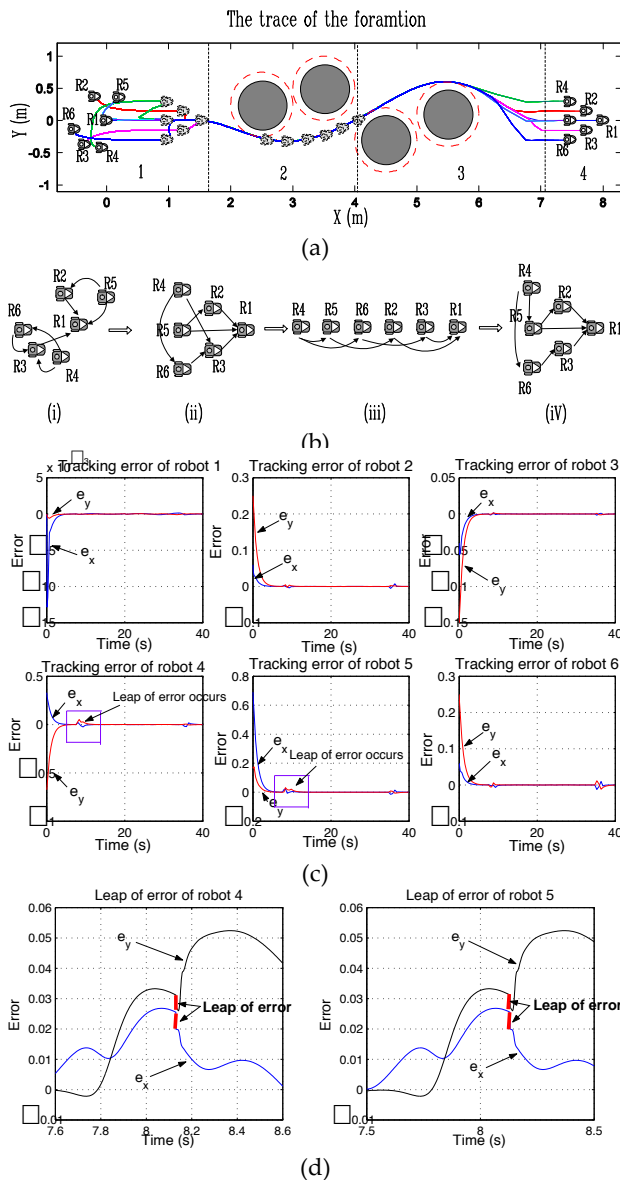


Fig. 8. Simulation results of the formation

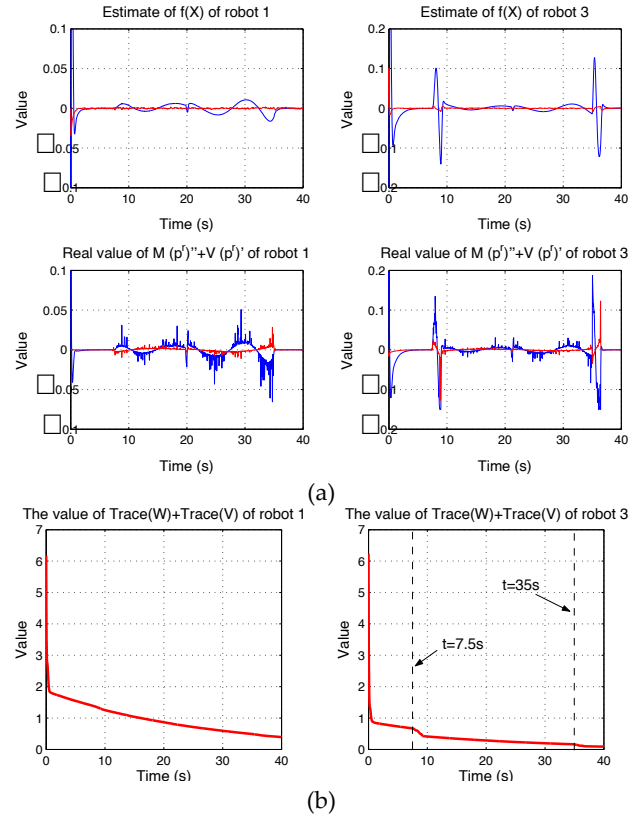


Fig. 9. Simulation results about adaptive NN convergence

## 6. Conclusions

As a kind of information consensus among mobile robots, formation control plays a very important role in formation navigation. This paper describes the relationship within formation in two aspects: formation pattern denoted by  $D^d$  and interaction topology graph described by the adjacency matrix  $G$ . Therefore  $G \circ D^d$  includes all relative information within a formation.

The relative position error is induced from the formation description. Suppose that there are unmodeled structures and bounded disturbance, a neural network control strategy with robust term is proposed in the paper for formation control. To apply the NN control strategy under all possible circumstances, such as variant or invariant formation pattern and interaction topology, the paper discusses the principles which should be satisfied in any design of formation navigation. In one word, if a formation pattern is of class  $C^k$  ( $k \geq 1$ ) and the interaction graph is connected and changed finite times, the formation control ensures that robots must form the formation with predetermined shape.

## 7. Appendix

### A.1. Proof of Lemma 1 :

Firstly we prove that given  $D^d$ , the desired relative position  $P^d$  is determined.

According to the definitions of  $P^d$  and  $D^d$ , we know that  $HP^d = G \circ D^d 1_{N \times 1}$ . There are two facts: 1) Because  $R_i$  is the

leader of the formation,  $g_{il}=1$ , while  $g_{ij}=0$  ( $j=1, \dots, N$ ,  $j \neq l$ ), and the entries in the  $l$ th row of  $H$  are zero; 2) Since  $D_{ii}=0$ , the  $l$ th element of  $G \circ D^d 1_{N \times 1}$  is zero too. Since  $p_l^d=0$ , the equation can be reduced to

$$\bar{H} \bar{P}^d = \bar{G} \circ \bar{D}^d 1_{N \times 1}, \quad (\text{A.1.1})$$

where  $\bar{P}^d = [p_1^d \ \dots \ p_{l-1}^d \ p_{l+1}^d \ \dots \ p_N^d]^T$ ,  $\bar{H}$  is the matrix resulting from taking off the  $l$ th row and the  $l$ th column of  $H$ ,  $\bar{G}$  and  $\bar{D}$  are the matrices resulting from taking off the  $l$ th rows of  $G$  and  $D$  respectively. Since  $\bar{H}$  is full rank, there is only one nonzero solution for (A.1.1). Hence if  $D^d$  is given, the relative position  $P^d$  is determined.

Therefore substituting  $P^d$  into (2) yields  $E = H(P - P^d)$ . If  $E = 0$ , we have  $H(P - P^d) = 0$ .

Secondly we investigate the property of  $H$ . If  $R_i$  is not

the formation leader, it holds that  $\sum_{j=1, j \neq i}^N |h_{ij}| = \sum_{j=1, j \neq i}^N |g_{ij}| = 1$ ,  $i=1, \dots, N$ . If  $R_i$  is the leader, then  $\forall j$ ,  $h_{ij}=0$ . According

to the Geršgorin discs theorem (Horn, R. A. & Johnson, C. R., 1985), we know that all eigenvalues of  $H$  are located within a unit circle with (1, 0) as its center. If the direct graph associated with  $G$  has a spanning tree, according to Corollary 1 in (Ren, W., Beard, R. W. & McLain, T. W., 2003),  $H$  has only one zero eigenvalue. Since  $G$  is a

stochastic matrix, it holds that  $\sum_{j=1}^N h_{ij} = 0$ , i.e.,  $H \cdot 1_{N \times 1} = 0$ .

That means the eigenvector corresponding to zero eigenvalue is 1. Therefore the kernel of  $H$  is  $\text{span}\{1\}$ .

Consequently it holds that  $(P - P^d) \in \text{span}\{1\}$ , so that all elements in the vector  $P - P^d$  are the same. That means if  $E$  converges to zero, the coordinates of robots have identical offsets relative to their desired positions in formation. Then all robots must form the formation described by formation pattern. Moreover because  $p_i^d \equiv 0$ , we have  $p_i = p_l + p_i^d$ ,  $i=1, \dots, N$ ,  $i \neq l$ .

#### A.2. Proof of Property 1:

According to Euclidean norm, we have

$$\|X\| = (\|p\|^2 + \|\dot{p}\|^2 + \cos^2 \theta + \sin^2 \theta)^{1/2}.$$

Since the following inequalities hold,

$$\|\dot{p}\|^2 = \|\dot{p}^d - \Lambda \dot{e}\|^2 \leq 2\|\dot{p}^d\|^2 + 2(\|\Lambda\| \|\dot{e}\|)^2,$$

$$\|\dot{p}^d\|^2 = \|\dot{p}^d - \Lambda e\|^2 \leq 2\|\dot{p}^d\|^2 + 2(\|\Lambda\| \|e\|)^2,$$

$\|p\|^2 = \|\Lambda^{-1}(z - \dot{e}) + p^d\|^2 \leq 4(\|\Lambda\|^{-1} \|z\|)^2 + 4(\|\Lambda\|^{-1} \|\dot{e}\|)^2 + 2\|p^d\|^2$ , we have

$$\begin{aligned} \|X\| &\leq \left[ 2\|p^d\|^2 + 2\|\dot{p}^d\|^2 + 2\|\dot{p}^d\|^2 + 4\|\Lambda\|^{-2} \|z\|^2 \right. \\ &\quad \left. + (2\|\Lambda\|^2 + 4\|\Lambda\|^{-2}) \|\dot{e}\|^2 + 2\|\Lambda\|^2 \|e\|^2 + 1 \right]^{1/2} \\ &\leq \sqrt{2}\Phi + 1 + 2\|\Lambda\|^{-1} \|z\| + \sqrt{2\|\Lambda\|^2 + 4\|\Lambda\|^{-2}} \|\dot{e}\| + \sqrt{2}\|\Lambda\| \|e\|. \end{aligned} \quad (\text{A.2.1})$$

According to property of BIBO system, if  $\|z\|$  is bounded, and  $e(0)$  and  $\dot{e}(0)$  are bounded,  $\|\dot{e}(t)\|$  and  $\|e(t)\|$  are always bounded, and  $\|\dot{e}(t)\|$  is growing as  $O(\|e(t)\|)$ . Therefore there are two positive constants,  $c_{m1}$  and  $c_{m2}$ , such that  $\|e(t)\| \leq c_{m1}$  and  $\|\dot{e}(t)\| \leq c_{m2}$ . Substituting it into (A.2.1), we have the bound of  $\|X\|$  as

$$\|X\| \leq c_1 \Phi + c_2 \|z\| + c_3, \quad (\text{A.2.2})$$

where  $c_3 = 1 + c_{m1} + c_{m2}$ . Due to  $\|\dot{z}\| = \|Tz\| = \|z\|$ , the property is obtained.  $\odot$

#### A.3. Proof of Property 2:

From (13), it holds that

$$O(\tilde{V}^T X)^2 = \sigma(V^T X) - \sigma(\hat{V}^T X) - \sigma'(\hat{V}^T X) \tilde{V}^T X.$$

Since  $\sigma(\cdot)$  and its derivative are bounded, there are two positive constants  $c_4$  and  $c_5$  such that

$$\begin{aligned} \|O(\tilde{V}^T X)^2\| &\leq \|\sigma(V^T X) - \sigma(\hat{V}^T X)\| + \|\sigma'(\hat{V}^T X) \tilde{V}^T X\| \\ &\leq c_4 + c_5 \|\tilde{V}^T X\|. \end{aligned} \quad (\text{A.3.1})$$

Substitute (10) into (A.3.1).

$$\begin{aligned} \|O(\tilde{V}^T X)^2\| &\leq c_4 + c_6 \Phi \|\tilde{V}\|_F + c_7 \|\tilde{V}\|_F + c_8 \|\tilde{V}\|_F \|\tilde{z}\| \\ &\leq c_4 + c_8 \|\tilde{V}\|_F \|\tilde{z}\| + c_9 \|\tilde{V}\|_F, \end{aligned} \quad (\text{A.3.2})$$

where  $c_6$  to  $c_9$  are positive scalars,  $c_9 = c_6 \Phi + c_7$ .

#### A.4. Proof of Theorem 1:

A Lyapunov function candidate is defined as

$$L = \frac{1}{2} [z^T M_c \tilde{z} + \text{tr}\{\tilde{W}^T F^{-1} \tilde{W}\} + \text{tr}\{\tilde{V}^T U^{-1} \tilde{V}\}]. \quad (\text{A.4.1})$$

Obviously  $L(0) = 0$ . If the robust term  $\gamma$  referred in (17) is of the form

$$\gamma = \begin{cases} -K_y (\|\hat{Y}\|_F + Y_M) \tilde{z} - J \frac{\tilde{z}}{\|\tilde{z}\|}, & \|\tilde{z}\| \neq 0 \\ -K_y (\|\hat{Y}\|_F + Y_M) \tilde{z}, & \|\tilde{z}\| = 0 \end{cases}, \quad (\text{A.4.2})$$

where  $J$  and  $K_y$  are positive, this robust term makes  $\tilde{z}$  be non-smooth but still Lipschitz continuous. According to Lyapunov theory for non-smooth system (Filippov, A. F., 1964, Ceragioli, F., 2002), the derivative of  $L$  is expressed as

$$\frac{d}{dt} L \stackrel{a.e.}{\in} \dot{\tilde{L}}, \quad (\text{A.4.3})$$

where  $\dot{\tilde{L}} = \bigcap_{\xi \in \partial L} \xi^T \begin{pmatrix} \mathbf{K}[f] \\ 1 \end{pmatrix}$ , where  $\mathbf{K}[f]$  represents the

Filippov solution of function  $f(\cdot)$ , which is defined as

$$\mathbf{K}[f](x, t) \equiv \bigcap_{\delta > 0} \bigcap_{\mu(N)=0} \overline{\text{co}} f(B(\tilde{z}, \tilde{W}, \tilde{V}, \delta) - N). \quad (\text{A.4.4})$$

In this paper,  $f(\cdot)$  is an equation set including (18) and (20). According to the definition,  $L$  has smooth partial derivative. Because of nonsmooth property of the robust term, the derivative of  $\tilde{L}$  is expressed as

$$\begin{aligned} \dot{\tilde{L}} &\subset -\tilde{z}^T K \tilde{z} + \text{tr}\{\tilde{W}^T (F^{-1} \dot{\tilde{W}} - \hat{\sigma} \tilde{z}^T + \hat{\sigma}' \hat{V}^T X \tilde{z}^T)\} \\ &\quad + \text{tr}\{\tilde{V}^T (U^{-1} \dot{\tilde{V}} - X \tilde{z}^T \hat{W}^T \hat{\sigma}') + \mathbf{K}[\tilde{z}^T (s + \gamma)]\}. \end{aligned} \quad (\text{A.4.5})$$

Since  $\dot{\tilde{W}} = -\hat{W}$  and  $\dot{\tilde{V}} = -\hat{V}$ , substituting (18) into (A.4.3) yields

$$\begin{aligned} \dot{\tilde{L}} \subset & -\tilde{z}^T K \tilde{z} + \kappa \|\tilde{z}\| \text{tr}\{\tilde{W}^T (W - \tilde{W})\} \\ & - \kappa \|\tilde{z}\| \text{tr}\{\tilde{V}^T (V - \tilde{V})\} + \mathbf{K}[\tilde{z}^T (s + \gamma)]. \end{aligned} \quad (\text{A.4.6})$$

It is denoted that  $Y = \text{diag}\{W, V\}$ ,  $\hat{Y} = \text{diag}\{\hat{W}, \hat{V}\}$ , and  $\tilde{Y} = Y - \hat{Y}$ . Then (A.4.6) can be expressed as

$$\dot{\tilde{L}} \subset -\tilde{z}^T K \tilde{z} + \kappa \|\tilde{z}\| \text{tr}\{\tilde{Y}^T (Y - \tilde{Y})\} + \mathbf{K}[\tilde{z}^T (s + \gamma)]. \quad (\text{A.4.7})$$

Substituting  $\gamma$  into (A.4.7), and considering that if  $\|\tilde{z}\| \neq 0$ ,

$\text{tr}\{\tilde{Y}^T (Y - \tilde{Y})\} = \langle \tilde{Y}, Y \rangle_F - \|\tilde{Y}\|_F^2 \leq \|\tilde{Y}\|_F \|Y\|_F - \|\tilde{Y}\|_F^2$ , yields

$$\begin{aligned} \dot{\tilde{L}} \leq & -K_{\min} \|\tilde{z}\|^2 + \kappa \|\tilde{z}\| (\|\tilde{Y}\|_F \|Y\|_F - \|\tilde{Y}\|_F^2) \\ & - K_Y (\|\hat{Y}\|_F + Y_M) \|\tilde{z}\|^2 - J \|\tilde{z}\| + \|\tilde{z}\| \|s\|, \end{aligned} \quad (\text{A.4.8})$$

where  $K_{\min}$  is the minimum singular value of  $K$ . The following property presents the bound of  $\|s(t)\|$  (Lewis, F. L., Yegildirek, A. & Liu, K., 1996).

*Property 3:* Based on Property 2, the disturbance term  $s(t)$  is bounded by

$$\|s(t)\| = C_0 + C_1 \|Y\|_F + C_2 \|\tilde{Y}\|_F \|\tilde{z}\|, \quad (\text{A.4.9})$$

where  $C_0$ ,  $C_1$  and  $C_2$  are positive scalars.

Substituting (A.4.9) into (A.4.8) yields

$$\begin{aligned} \dot{\tilde{L}} \leq & -K_{\min} \|\tilde{z}\|^2 + \kappa \|\tilde{z}\| (\|\tilde{Y}\|_F \|Y\|_F - \|\tilde{Y}\|_F^2) \\ & - K_Y (\|\hat{Y}\|_F + Y_M) \|\tilde{z}\|^2 + \|\tilde{z}\| (C_0 + C_1 \|\tilde{Y}\|_F + C_2 \|\tilde{Y}\|_F \|\tilde{z}\|) - J \|\tilde{z}\|, \end{aligned} \quad (\text{A.4.10})$$

If  $K_Y$  is designed such that  $K_Y > C_2$ , and due to the fact that  $\|\hat{Y}\|_F + Y_M \geq \|\hat{Y}\|_F + \|Y\|_F \geq \|Y - \hat{Y}\|_F = \|\tilde{Y}\|_F$ , we can obtain

$$\begin{aligned} \dot{\tilde{L}} \leq & -K_{\min} \|\tilde{z}\|^2 + \kappa \|\tilde{z}\| (\|\tilde{Y}\|_F \|Y\|_F - \|\tilde{Y}\|_F^2) + \|\tilde{z}\| (C_0 + C_1 \|\tilde{Y}\|_F) - J \|\tilde{z}\| \\ \leq & -\|\tilde{z}\| [K_{\min} \|\tilde{z}\| - \kappa \|\tilde{Y}\|_F (Y_M - \|\tilde{Y}\|_F) - C_0 - C_1 \|\tilde{Y}\|_F + J] \\ = & -\|\tilde{z}\| [K_{\min} \|\tilde{z}\| + \kappa (\|\tilde{Y}\|_F - \frac{C_3}{2})^2 - \frac{\kappa C_3^2}{4} - C_0 + J], \end{aligned} \quad (\text{A.4.11})$$

where  $C_3 = Y_M + \frac{C_1}{\kappa}$ . Obviously if we take  $J \geq \frac{\kappa C_3^2}{4} + C_0$ , it follows that

$$\dot{\tilde{L}} \leq -\|\tilde{z}\| [K_{\min} \|\tilde{z}\| + \kappa (\|\tilde{Y}\|_F - \frac{C_3}{2})^2] \leq 0. \quad (\text{A.4.12})$$

Hence (A.4.1) is a Lyapunov function. According to the structure of (A.4.1),  $\tilde{z}$ ,  $\tilde{W}$ , and  $\tilde{V}$  are bounded. Then by LaSalle's principle for nonsmooth system (Shevitz, D. & Paden, B., 1994), the system must stabilize to the invariant set enclosed in  $\{\tilde{z} | \dot{\tilde{V}} = 0\}$ , where  $\tilde{z} = 0$ . Since the determinant of  $T$  is one, it holds  $z = T^{-1} \tilde{z} = 0$  when  $\tilde{z} = 0$ . Therefore  $e$  and  $\dot{e}$  converge to zero, and in the end

$p_i = \sum_{j=1}^N g_{ij} (p_j + D_{ij}^d)$ . Hence the NN control law with

robust term can make robot follow reference point with no errors. Since the individual error results from (2), according to Lemma 1, it is concluded that robots must form the formation described by  $D^d$ .

#### A.5. Proof of Theorem 2:

Obviously the dynamics equations of the system include (18) and (20). If  $D^d(t) \in C^k$ ,  $k \geq 2$ , the second order derivative of  $D^d(t)$  is Lipschitz continuous, so that (18) and (20) are Lipschitz, and the proof of convergence is the same as the previous subsection. So here we need to prove the formation stability under the assumption that  $D^d(t) \in C^1$  functions. This assumption is very useful for formation pattern generation, which will be illustrated in the simulation later. Since we assume  $D^d(t)$  is of class  $C^1$ ,  $\dot{D}^d(t)$  is Lipschitz continuous, and the second order derivative of  $D^d(t)$  is bounded.

According to the definition of sigmoid function,  $\sigma(x) = \frac{1}{1+e^{-x}}$ , it holds that  $\forall x \in R$ ,  $\|\sigma(x)\| \in [0, 1]$ . And its derivative satisfies  $\|\sigma'(x)\| \in [0, \frac{1}{4}]$ . All parameters referred in (17) and (18), including  $F$ ,  $U$ ,  $\kappa$ ,  $\bar{\tau}_d$  and  $\varepsilon$ , are bounded. Therefore to make the dynamics functions (18) and (20) be locally bounded functions, the key precondition is that  $X_i = [\dot{p}_i \sin \theta_i \cos \theta_i \ddot{p}_i^r \dot{p}_i^r]^T$  is bounded. According to the definition of  $p_i^d$ , for robot  $i$ , Property 1 is expressed as

$$\|X_i\| \leq c_1 \bar{\Phi}_i + c_2 \|\tilde{z}_i\| + 1 + \sum_{j=1}^N g_{ij} (\|p_j\| + \|\dot{p}_j\| + \|\ddot{p}_j\|), \quad (\text{A.5.1})$$

where  $\bar{\Phi}_i$  satisfies

$$\left\| \begin{aligned} & \sum_{j=1}^N g_{ij} D_{ij}^d \\ & \sum_{j=1}^N g_{ij} \dot{D}_{ij}^d \\ & \sum_{j=1}^N g_{ij} \ddot{D}_{ij}^d \end{aligned} \right\| \leq \bar{\Phi}_i. \quad (\text{A.5.2})$$

Obviously, to make  $X_i$  be locally bounded, the positions of  $R_i$ 's leaders,  $p_j$ , where  $g_{ij} \neq 0$ , should be at least belong to class  $C^1$ .

Assume that  $X_i$  is bounded, then (18) and (20) are locally bounded functions. According to the properties of integral, for a finite interval of time  $[0, t]$ ,  $t < \infty$ ,  $\tilde{z}_i(t)$ ,  $\hat{W}_i(t)$  and  $\hat{V}_i(t)$  are Lipschitz continuous. From the definition of the filter error  $\tilde{z}_i$ , we know the position of robot  $p_i(t)$  is smooth continuous. Considering all robots, it is concluded that if initial coordinate  $p_i(0)$  is finite, after a finite interval of time  $[0, t]$ ,  $X_i(t)$  is bounded.

Then (18) and (20) are locally bounded. And both equations can be expressed in Filippov sense. Since  $\tilde{z}$ ,  $\hat{W}$  and  $\hat{V}$  are Lipschitz continuous, the following expressions hold.

$$\dot{\hat{W}} \in F \cdot \mathbf{K} [\hat{\sigma} \hat{V}^T X \tilde{z}^T - F \hat{\sigma} \tilde{z}^T] - \kappa F \|\tilde{z}\| \hat{W} \quad (\text{A.5.3})$$

$$\dot{\hat{V}} \in -U \cdot \mathbf{K} [X (\hat{\sigma}^T \hat{W} \tilde{z})^T] - \kappa U \|\tilde{z}\| \hat{V}. \quad (\text{A.5.4})$$

$$\begin{aligned} \dot{\tilde{z}} \in & -M_c^{-1} K \tilde{z} - M_c^{-1} \cdot \mathbf{K} [\tilde{W}^T (\hat{\sigma} - \hat{\sigma} \hat{V}^T X) - \hat{W}^T \hat{\sigma} \hat{V}^T X + s + M_c^{-1} \gamma], \\ & (\text{A.5.5}) \end{aligned}$$

If the same Lyapunov candidate shown in (A.4.1) is chosen, the following equation shows that if  $D^d(t) \in C^1$ , the variant  $D^d(t)$  will not change the convergence of control strategy.

$$\begin{aligned}
\dot{L} &= \dot{z}^T M_c \dot{z} + tr\{\tilde{W}^T F^{-1} \dot{\tilde{W}}\} + tr\{\tilde{V}^T U^{-1} \dot{\tilde{V}}\} \\
&\leq -\dot{z}^T M_c^{-1} K \dot{z} + tr\{\tilde{W}^T (F^{-1} \dot{\tilde{W}} - K[\hat{\sigma} \dot{z}^T - \hat{\sigma}' \hat{V}^T X \dot{z}^T])\} \\
&\quad + tr\{\tilde{V}^T (U^{-1} \dot{\tilde{V}} - K[X \dot{z}^T \hat{W}^T \hat{\sigma}'])\} + \dot{z}^T (K[s + \gamma]) \\
&\leq -\dot{z}^T M_c^{-1} K \dot{z} + tr\{\tilde{W}^T (K[\hat{\sigma} \dot{z}^T - \hat{\sigma}' \hat{V}^T X \dot{z}^T] \\
&\quad - K[\hat{\sigma} \dot{z}^T - \hat{\sigma}' \hat{V}^T X \dot{z}^T])\} + tr\{\tilde{V}^T (K[X(\hat{\sigma}'^T \hat{W} \dot{z})^T \\
&\quad - K[X(\hat{\sigma}'^T \hat{W} \dot{z})^T])\} + \kappa F \|\dot{z}\| tr\{\tilde{W} \dot{W}\} \\
&\quad + \kappa U \|\dot{z}\| tr\{\tilde{V} \dot{V}\} + \dot{z}^T (K[s + \gamma]) \\
&= -\dot{z}^T K \dot{z} + \kappa \|\dot{z}\| tr\{\tilde{W}^T (W - \tilde{W})\} \\
&\quad - \kappa \|\dot{z}\| tr\{\tilde{V}^T (V - \tilde{V})\} + \dot{z}^T (K[s + \gamma])
\end{aligned} \quad (A.5.6)$$

Since  $X_i$  is bounded in the case of smooth continuous  $D^d(t)$ , Property 2 and Property 3 still hold. Therefore (A.5.6) is almost the same as (A.4.6). Hence the following proof and the values of parameters are similar to the previous subsection, and the convergence of formation control is guaranteed.

#### A.6. Proof of Theorem 3:

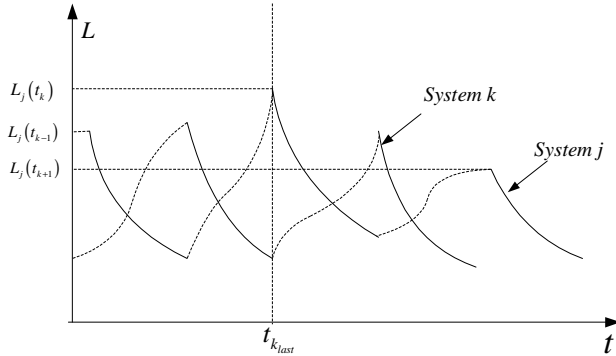


Fig. A.6.1. Stability of a switched system. Solid/dashed line denotes corresponding system active/inactive. If there are finite times of increasing  $L_j(t_k)$ , there is  $t_{k_{last}}$ , such that all  $k \geq k_{last}$ ,  $L_j(t_{k+1}) > L_j(t_k)$

The proof is almost the same as the proof about Theorem 2.3 in (Branicky, M. S., 1998) except the following differences.

- 1) Since  $S|j$  is not strictly increasing but nondecreasing sequence, sequence  $S|j$  may have the sequence of switching times in which some adjacent times are the same. For example  $\pi_2(S|j) = x_0, t_0, t_1, t_1, t_2, \dots$ . This property implies that there is a kind switch not changing index of system, i.e. the systems in both adjacency intervals are the same. But this does not affect the proof of stability.
- 2) Property 2) of  $L_j$  implies that there exist finite times such that  $L_j(t_{k+1}) > L_j(t_k)$ , where  $t_k \in \mathcal{E}(S|j)$ . If  $L_j(t_0)$  is bounded, there is  $k_{max}$  such that  $L_j(t_{k_{max}})$  denotes the

maximum of  $L_j(t_k)$ ,  $t_k \in \mathcal{E}(S|j)$ . Hence  $L_j(t_k)$  must be bounded. Moreover since there are finite times  $t_k$  on which  $L_j(t_{k+1}) > L_j(t_k)$ ,  $t_k \in \mathcal{E}(S|j)$ , after the last time of increasing, denoted by  $k_{last}$ , the subsequence of  $S|j$  after  $t_{k_{last}}$  denoted by  $S_{k_{last}}|j$  must be monotonically nonincreasing. Then the stability of the switched system in Lyapunov sense is guaranteed using similar method in (Branicky, M. S., 1998). Fig. A.6.1 depicts this finite increasing  $L_j(t_k)$  over time.  $\odot$

## 8. References

- Vicsek, T.; Czirok, A.; Jacob, E. B. & Schochet, O. (1995). Novel Type of Phase Transitions in a System of Self-driven Particles. *Phys. Rev. Lett.*, Vol. 75, 1995, pp. 1226-1229
- Jababai, A.; Lin, J. & Morse, A. S. (2003). Coordination of Groups of Mobile Autonomous Agents Using Nearest Neighbor Rules. *IEEE Trans. Autom. Control*, Vol. 48, No. 6, 2003, pp. 988-1001
- Ren, W. & Beard, R. W. (2005). Consensus Seeking in Multi-Agent Systems under Dynamically Changing Interaction Topologies. *IEEE Trans. Autom. Control*, Vol. 50, No. 5, 2005, pp. 655-661
- Wang, P. K. C. (1991). Navigation Strategies for Multiple Autonomous Mobile Robots Moving in Formation. *J. Robot. Syst.*, Vol. 8, No. 2, 1991, pp. 177-195
- Sugar, T. & Kumar, V. (1998). Decentralized control of cooperating mobile manipulators, *Proceedings of IEEE Int. Conf. Robot. Automat.*, pp. 2916-2921, 1998, Leuven, Belgium
- Desai, J. P.; Ostrowski, J. & Kumar, V. (1998). Controlling Formations of Multiple Mobile Robots. *Proceedings of IEEE Int. Conf. on Robotics and Automation*, pp. 2864-2869, 1998, Leuven, Belgium
- Lewis, M. A. & Tan, K.H. (1997). High Precision Formation Control of Mobile Robots Using Virtual Structures. *Autonomous Robot.*, Vol. 4, 1997, pp. 387-403
- Moscovitz, Y. & DeClaris, N. (1998). Basic Concepts and Methods for Keeping Autonomous Ground Vehicle Formations. *Proceedings of IEEE ISIC/CIRA/ISAS Joint Conf.*, pp. 44-49, 1998, Gaithersburg, MD
- Tan, K. H. & Lewis, M. A. (1996). Virtual Structures for High-Precision Cooperative Mobile Robotic Control. *Proceedings of the 1996 IEEE/RSJ Int. Conf. on Intelligent Robots and Systems*, pp. 132-139, 1996, Osaka, Japan
- Spry, S. C. (2002). Modeling and Control of Vehicle Formations, *PhD Thesis*, University of California, Berkeley, 2002
- Spry, S. & Hedrick, J. K. (2004). Formation Control Using Generalized Coordinates. *Proceedings of 43rd IEEE Conf. on Decision and Control*, pp. 2441-2446, 2004, Atlantis, Paradise Island, Bahamas

- Jonathan, R. T.; Beard, R. W. & Young, B. J. (2003). A Decentralized Approach to Formation Maneuvers. *IEEE Trans. Robot. and Automat.*, Vol. 19, 2003, pp. 933-941
- Balch, T. & Arkin, R. C. (1998). Behavior-Based Formation Control for Multirobot Teams, *IEEE Trans. Robot. Automat.*, Vol. 14, 1998, pp. 926-939
- Chen, Q. & Luh, J. Y. S. (1994). Coordination and Control of a Group of Small Mobile Robots, *Proceedings of IEEE Int. Conf. on Robotics and Automation*, pp. 2315-2320, 1994
- Schneider, F. E. & Wildermuth, D. (2003). A Potential Field Based Approach to Multi Robot Formation Navigation. *Proceedings of the IEEE Int. Conf. on Robotics, Intelligent Systems and Signal Processing*, pp. 680-685, 2003, Changsha, China
- Tanner, H. G.; Pappas, G. J. & Kumar, V. (2004). Leader-to-Formation Stability. *IEEE Trans. Rob. Autom.* Vol. 20, No. 3, 2004, pp. 443-455
- Liu, Y.; Passino, K. M. & Polycarpou, M. (2001). Stability Analysis of One-Dimensional Asynchronous Swarms. *Proceedings of American Control Conf.*, pp. 716-721, 2001, Arlington, VA
- Ogren, P.; Egerstedt, M. & Hu, X. (2002). A Control Lyapunov Function Approach to Multi-Agent Coordination. *IEEE Trans. Rob. Autom.*, Vol. 18, No. 5, 2002, pp. 847-851
- Kowalczyk, W. & Kozlowski, K. (2004). Artificial Potential Based Control for a Large Scale Formation of Mobile Robots. *Proceedings of The 4th Int. Workshop on Robot Motion and Control*, pp. 285-291, 2004
- Bicho, E. & Monteiro, S. (2003). Formation Control for Multiple Mobile Robots: a Non-linear Attractor Dynamic Approach. *Proceedings of 2003 IEEE/RSJ Int. Conf. on Intelligent Robots and Systems*, pp. 2016-2022, 2003, Las Vegas, NV
- Balch, T. & Hybinette, M. (2000). Social Potentials for Scalable Multi-robot Formations. *Proceedings of IEEE Int. Conf. on Robotics and Automation*, pp. 73-80, 2000, San Francisco, USA
- Fierro, R. & Lewis, F. L. (1998). Control of a Nonholonomic Mobile Robot Using Neural Networks. *IEEE Trans. Neural Networks*, Vol. 9, No. 4, 1998, pp. 589-600
- Lewis, F. L.; Yegildirek, A. & Liu, K. (1996). Multilayer Neural-Net Robot Controller with Guaranteed Tracking Performance. *IEEE Trans. Neural Networks*, Vol. 7, No. 2, 1996, pp. 388-399
- Li, Y. & Chen, X. (2005). Leader-Formation Navigation with Sensor Constraints. *Proceedings of IEEE Int. Conf. on Information Acquisition*, pp. 554-559, 2005, Hongkong and Macau, China
- Horn, R. A. & Johnson, C. R. (1985). *Matrix Analysis*, Cambridge University Press.
- Ren, W.; Beard, R. W. & McLain, T. W. (2003). Coordination Variables and Consensus Building in Multiple Vehicle Systems. *Proceedings of the Block Island Workshop on Cooperative Control*, Springer-Verlag Series: Lecture Notes in Control and Information Sciences, Vol. 309, pp. 171-188, 2003
- Filippov, A. F. (1964). Differential Equation with Discontinuous Right-Hand Side. *Amer. Math. Soc. Trans.*, Vol. 42, No. 2, 1964, pp. 191-231
- Ceragioli, F. (2002). Some Remarks on Stabilization by Means of Discontinuous Feedbacks. *Systems and Control Letters*, Vol. 45, No. 4, 2002, pp. 271-281
- Shevitz, D. & Paden, B. (1994). Lyapunov Stability Theory of Nonsmooth Systems. *IEEE Trans. Autom. Control*, Vol. 39, No. 9, 1994, pp. 1910-1914
- Branicky, M. S. (1998). Multiple Lyapunov Functions and Other Analysis Tools for Switched and Hybrid Systems. *IEEE Trans. Autom. Control*, Vol. 43, No. 4, 1998, pp. 475-482